PHYSICAL REVIEW B **83**, 140503(R) (2011)

Theory of an inherent spin-density-wave instability due to vortices in superconductors with strong Pauli effects

Kenta M. Suzuki, Masanori Ichioka, and Kazushige Machida
Department of Physics, Okayama University, Okayama 700-8530, Japan
(Received 17 January 2011; revised manuscript received 8 March 2011; published 8 April 2011)

A spin-density-wave (SDW) instability mechanism enhanced by vortices under fields is proposed to explain the high field and low-temperature phase in $CeCoIn_5$. In the vortex state strong Pauli effect and nodal gap conspire to enhance the momentum-resolved density of states over the normal state value exclusively along the nodal direction, providing a favorable nesting condition for SDW with $\mathbf{Q} = (2k_F, 2k_F, 0.5)$ only at high fields (H). We can consistently understand observed mysteries of the field-induced SDW confined below H_{c2}, such as facts that $\mathbf{Q}$ is directed to the nodal direction independent of H, SDW diminishes under tilting field from the ab plane, and the SDW transition line in (H,T) has a positive slope.

DOI: 10.1103/PhysRevB.83.140503 PACS number(s): 74.70.Tx, 74.25.Uv, 74.20.−z

Competing-order phenomena are a hallmark of strongly correlated systems. This is particular true for superconductors such as in heavy fermion materials, high T_c cuprates, or pnictides, where an spin-density-wave (SDW) order generically competes or coexists with superconductivity (SC),[1–3] because competing magnetism is deeply related to the pairing mechanism itself. Thus it is not entirely surprising to see that applied field induces an SDW in superconductors. In fact, in $La_{1-x}Sr_xCuO_4$ and $CeRhIn_5$ under pressures,[4,5] the field-induced SDW is observed only for finite fields and is absent at zero field. A remarkable observation in the high field and low-temperature (HL) phase of a heavy fermion superconductor $CeCoIn_5$ is that the induced SDW is confined exclusively in the superconducting state below the upper critical field H_{c2} [see HL in Fig. 3(c)].[1]

Since Abrikosov's work[6] there have been many studies on vortices in type II superconductors, based on a concept that the vortex core is a featureless rigid cylindrical object filled with normal electrons. A concept based on microscopic Bogoliubov–de Gennes or quasi-classical Eilenberger framework is recently revealing far richer quasiparticle (QP) structures both in real space and reciprocal space, which govern a variety of physical characteristics in type II superconductors under fields.[7] In particular, in a superconductor characterized by an anisotropic gap, including a nodal gap such as a d-wave symmetry, the QP spatial structure is directly or indirectly measured by various experimental methods such as scanning tunnel microscope (STM) as direct spatial images,[8] small angle neutron scattering (SANS) as Fourier-transformed images,[9] or field-angle resolved specific heat[10] or thermal conductivity.[11] With this emergent QP concept we would expect to uncover new phenomena.

Here we investigate detailed behaviors of QPs induced by vortices in superconductors with nodal gap structure (i.e., $d_{x^2-y^2}$) and strong Pauli paramagnetic effect to uncover the origin of the HL phase in $CeCoIn_5$. This has been discussed theoretically from different points of view.[12–16] We find generic features of the QP behavior, which gives us a clear physical picture, and synthesizes complementary information in real space and reciprocal space. This picture, in particular in reciprocal space, clarifies reasons for SDW instability in high fields confined at $H < H_{c2}$. The duality of the QP behaviors in real and reciprocal space is a key concept in uncovering the origin of the HL phase. Note that the dHvA effect in the superconducting state the QPs executing the cyclotron motion in real space carry information about the original Fermi surface topology, proving the dual nature of the QPs created around the vortex core.

The mysterious HL phase exists for both H applied to the basal plane ($H \parallel ab$)[17–22] and the c axis ($H \parallel c$)[23] of the tetragonal crystal. In particular, for the $H \parallel ab$ case the mounting evidence[2,3] shows that an SDW characterizes the HL phase. The HL phase [see Fig. 3(c)] appears via a second-order phase transition $H_Q(T)$ from the conventional Abrikosov vortex lattice state. Namely the sublattice magnetization of SDW grows continuously at $H_Q(T)$ and disappears abruptly at H_{c2} via a first-order transition. The ordering wave vector $Q = (0.45, 0.45, 0.5)$ in the reciprocal units is independent of the field directions $H \parallel (1\bar{1}0)$[2] and $H \parallel (100)$,[3] and independent of the field strength. The phase boundary $H_Q(T)$ between the HL and the Abrikosov state is almost independent of two field directions. $H_Q(T)$ is an increasing function of T. These features are observed mainly by the neutron scattering experiments,[2,3] and basically are consistent with other thermodynamic measurements[17] and NMR experiments.[19,20] Since the pairing symmetry of this material is firmly established as $d_{x^2-y^2}$ type,[10,11] the origin of this HL phase must be tied to (1) the d-wave nature of this system and (2) the vortex state under a field. As for (1) the controversy of the pairing symmetry either $d_{x^2-y^2}$ or d_{xy} is now resolved,[11,24] and there is little doubt of the $d_{x^2-y^2}$ symmetry in $CeCoIn_5$.[10] As for (2) it is known by SANS experiments[9] and by NMR experiments[19] that the Pauli paramagnetic effect is indispensable in understanding the anomalous behaviors of the scattering form factor as a function of H and T. The purpose of this paper is to examine the generic mechanism of SDW instability enhanced by the presence of vortices under the strong paramagnetic effect with d-wave pairing and two-dimensional Fermi surface. The Stoner instability of SDW can be investigated by examining the density of states (DOS) at the nesting point on the Fermi surface.

We calculate the spatial structure of the vortex lattice state in the clean limit by quasiclassical Eilenberger theory, which is valid for $k_F\xi \gg 1$ (k_F is the Fermi wave number

and ξ is the superconducting coherence length).[7] The Pauli paramagnetic effects are included through the Zeeman term $\mu_B B(\mathbf{r})$, where $B(\mathbf{r})$ is the flux density of the internal field and μ_B is a renormalized Bohr magneton. The quasiclassical Green's functions $g(\omega_n + i\mu B,\mathbf{k},\mathbf{r})$, $f(\omega_n + i\mu B,\mathbf{k},\mathbf{r})$, and $f^\dagger(\omega_n + i\mu B,\mathbf{k},\mathbf{r})$ are calculated in the vortex lattice state by the Eilenberger equations

$$\begin{aligned}[\omega_n + i\mu B + \tilde{\mathbf{v}}\cdot(\nabla + i\mathbf{A})]f &= \Delta\phi g,\\ [\omega_n + i\mu B - \tilde{\mathbf{v}}\cdot(\nabla - i\mathbf{A})]f^\dagger &= \Delta^*\phi^* g,\end{aligned} \tag{1}$$

where $g = (1 - ff^\dagger)^{1/2}$, $\mathrm{Re}\, g > 0$, $\tilde{\mathbf{v}} = \mathbf{v}/v_{F0}$, and the Pauli paramagnetic parameter $\mu = \mu_B B_0/\pi k_B T_c$. $\mathbf{k} = (k_a,k_b,k_c)$ is the relative momentum of the Cooper pair and $\mathbf{r}$ is the center-of-mass coordinate of the pair. We set the pairing function $\phi(\mathbf{k}) = \sqrt{2}(k_a^2 - k_b^2)/(k_a^2 + k_b^2)$ in $d_{x^2-y^2}$-wave pairing. We use the Eilenberger units R_0 and B_0.[25] The energy E, pair potential Δ, and Matsubara frequency ω_n are in units of $\pi k_B T_c$.

The averaged Fermi velocity $v_{F0} = \langle v^2\rangle_{\mathbf{k}}^{1/2}$, where $\langle\cdots\rangle_{\mathbf{k}}$ indicates the Fermi surface average. To model the quasi-two-dimensional Fermi surface of $CeCoIn_5$ we use a Fermi surface with a warped cylinder shape coming from the so-called α-Fermi surface [see four cylinders in Fig. 3(a)] [26] and the Fermi velocity is given by $\mathbf{v} = (v_a,v_b,v_c) \propto (\cos\theta_k, \sin\theta_k, \tilde{v}_z \sin k_c)$ at the Fermi surface $\mathbf{k} \propto (k_{F0}\cos\theta_k, k_{F0}\sin\theta_k, k_c)$ with $-\pi \leqslant \theta_k \leqslant \pi$ and $-\pi \leqslant k_c \leqslant \pi$. We set $\tilde{v}_z = 0.5$, thus the anisotropy ratio $\gamma = \xi_c/\xi_{ab} \sim \langle v_c^2\rangle_{\mathbf{k}}^{1/2}/\langle v_a^2\rangle_{\mathbf{k}}^{1/2} \sim 0.5$ as observed in $CeCoIn_5$.

As for self-consistent conditions, the pair potential is calculated by

$$\Delta(\mathbf{r}) = g_0 N_0 T \sum_{0<\omega_n\leqslant\omega_{\mathrm{cut}}} \langle\phi^*(\mathbf{k})(f + f^{\dagger *})\rangle_{\mathbf{k}} \tag{2}$$

with $(g_0 N_0)^{-1} = \ln T + 2T\sum_{0<\omega_n\leqslant\omega_{\mathrm{cut}}} \omega_n^{-1}$. We use $\omega_{\mathrm{cut}} = 20 k_B T_c$. The vector potential for the internal magnetic field is self-consistently determined by

$$\nabla\times(\nabla\times\mathbf{A}) = \nabla\times\mathbf{M}_{\mathrm{para}}(\mathbf{r}) - \frac{2T}{\kappa^2}\sum_{0<\omega_n}\langle\tilde{\mathbf{v}}\,\mathrm{Im}\;g\rangle_{\mathbf{k}}, \tag{3}$$

where we consider both the diamagnetic contribution of supercurrent in the last term and the contribution of the paramagnetic moment $\mathbf{M}_{\mathrm{para}}(\mathbf{r}) = [0,0,M_{\mathrm{para}}(\mathbf{r})]$ with

$$M_{\mathrm{para}}(\mathbf{r}) = M_0\left[\frac{B(\mathbf{r})}{H} - \frac{2T}{\mu H}\sum_{0<\omega_n}\langle\mathrm{Im}\;g\rangle_{\mathbf{k}}\right]. \tag{4}$$

The normal state paramagnetic moment $M_0 = (\mu/\kappa)^2 H$, $\kappa = B_0/\pi k_B T_c\sqrt{8\pi N_0}$, and N_0 is the DOS at the Fermi energy in the normal state. We set the Ginzburg-Landau parameter $\kappa = 89$. We solve Eqs. (1) and (2)–(4) alternately, and obtain self-consistent solutions as in previous works[7] under a given unit cell of the vortex lattice.

The local DOS in real space (r-DOS) is given by $N(\mathbf{r},E) = N_\uparrow(\mathbf{r},E) + N_\downarrow(\mathbf{r},E)$, where $N_\sigma(\mathbf{r},E) = \langle N_\sigma(\mathbf{r},\mathbf{k},E)\rangle_{\mathbf{k}} = N_0\langle\mathrm{Re}[g(\omega_n + i\sigma\mu B,\mathbf{k},\mathbf{r})|_{i\omega_n\to E+i\eta}]\rangle_{\mathbf{k}}$ with $\sigma = 1$ (-1) for the up (down) spin component. We typically use $\eta = 0.01$. The total DOS is obtained by the spatial average of the r-DOS as $N(E) = N_\uparrow(E) + N_\downarrow(E) = \langle N(\mathbf{r},E)\rangle_{\mathbf{r}}$. The momentum-resolved DOS (k-DOS) in reciprocal space is given by $N(\mathbf{k},E) = N_\uparrow(\mathbf{k},E) + N_\downarrow(\mathbf{k},E)$ as $N_\sigma(\mathbf{k},E) = \langle N_\sigma(\mathbf{r},\mathbf{k},E)\rangle_{\mathbf{r}}$. Those r-DOS and k-DOS are complementary, giving rise to valuable information about the QP structures in the vortex state.

We show the r-DOS at $E = 0$ in Fig. 1(a) and the corresponding k-DOS in Figs. 1(b) and 1(c) for $H \parallel (110)$ (left column) and $H \parallel (100)$ (right column) for large paramagnetic effect $\mu = 2$. In Fig. 1(a) we see several characteristic and eminent QP trajectories, notably the bands of the zero-energy

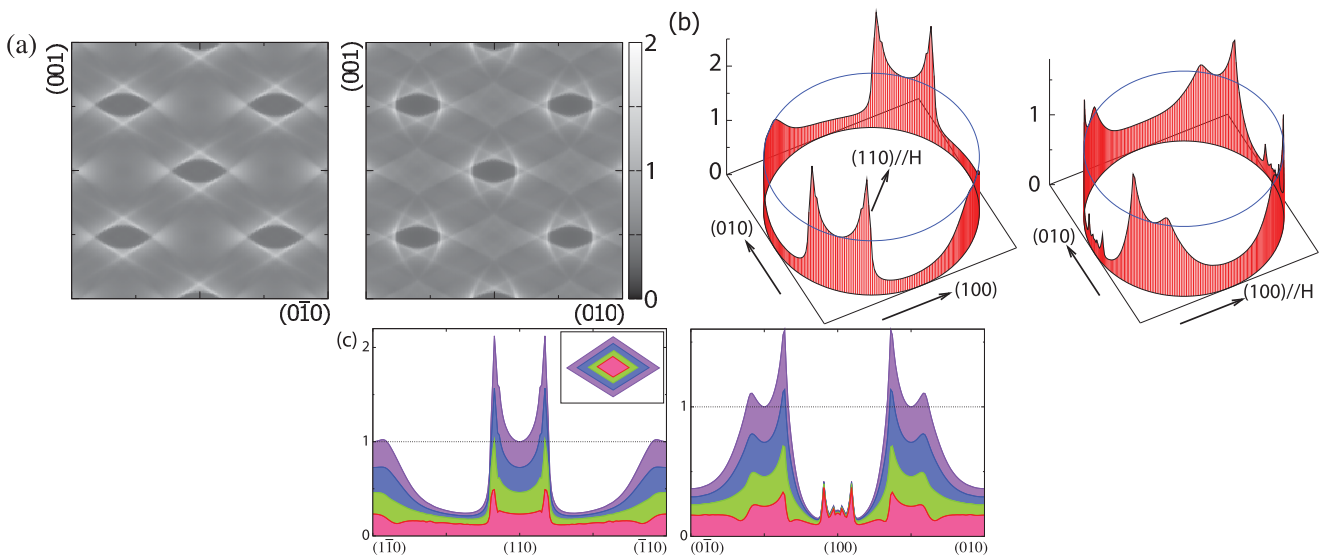

FIG. 1. (Color online) (a) r-DOS $N(\mathbf{r},E=0)/N_0$ in the real space of area 16×16 in the Eilenberger unit. Vortex cores are placed at the center of each black spot. (b) k-DOS $N(\mathbf{k},E=0)/N_0$ at $k_z = 0$ on the Fermi surface. Height of the upper rings indicates the normal state value N_0. (c) k-DOS is resolved into the contributed real space areas divided in a unit cell as shown by colors (gray scale) in the inset. Left column is for $H \parallel (110)$ and right for $H \parallel (100)$. $H/H_{c2} = 0.86$, $T/T_c = 0.05$, and $\mu = 2$.

DOS connecting the nearest neighbor vortex cores. Those real space trajectories correspond to the real space motions of the QP induced by H. It is seen that the zero-energy r-DOS is depleted at the vortex core, and piles up in the surrounding area because of the Pauli effect. Due to the Zeeman shift, zero-energy peak of r-DOS at the vortex core moves up and down in the energy, resulting in the depletion of the zero-energy DOS at the core, that is, the empty core.[25] The zero-energy state moves outside from the core where its maxima occurs. Figure 1(b) shows the corresponding k-DOS for each **k** direction on the Fermi circle at $k_z = 0$. The k-DOS enhancement along the nodal directions and strong suppression along the antinodal directions are clearly seen for both field orientations. This comes from the real space area surrounding the core, which is seen from Fig. 1(c) where the contribution to the k-DOS is resolved in the local areas (see inset) with the same areal size. The core area (the central region of the inset) gives a minor contribution because of the empty core.

The field evolutions of the k-DOS are shown in Fig. 2(a) for $H \parallel (110)$ with the strong Pauli effect. As H increases toward H_{c2} the k-DOS grows, keeping uneven distribution on the Fermi circle, namely the k-DOS is dominated along the nodal direction and suppressed along the antinodal direction. Upon increasing H, the total DOS in the vortex state increases toward the normal state value N_0 at H_{c2}. Because of the Pauli effect, even near H_{c2} the order parameter is not seriously suppressed. Thus beyond a certain H the enhanced k-DOS can exceed N_0. It is contrasted with the case of no Pauli effect ($\mu = 0$) [shown in Fig. 2(b)] where the order parameter decreases continuously via a second-order transition at H_{c2}. There the k-DOS never exceeds N_0, and the k-DOS enhancement never occurs even approaching H_{c2}. Thus the Pauli paramagnetic effect triggers the SDW instability by enhancing the nesting condition. The k-DOS enhancement occurs because under the in-plane field the QP diamagnetic motions are parallel to the k_z axis, thus they are sensing the nodal lines running along it, giving rise to the singularities in the k-DOS as seen in Fig. 2(a). This one-dimensional QP motion along the nodal line never appears when $H \parallel (001)$ as seen below.

In Fig. 2(c) we display the k-DOS for $H \parallel (001)$. The k-DOS distribution is featureless, because the QP trajectories in this field orientation traverse the perpendicular nodal line, yielding weakened singularities in the k-DOS. There is no k-DOS enhancement above N_0 for any values of H, implying that the SDW instability is absent in this orientation. Thus by tilting away from $H \parallel (110)$ toward (001) the k-DOS enhancement ceases to exist. According to our calculation, the critical tilting angle $\theta_{cr} \sim 30^\circ$ from the ab plane. Up to this angle the peak intensity of the k-DOS is maintained. According to Correa *et al.*[27] the HL phase disappears above $\theta \sim 30^\circ$.

In Fig. 3(a) we display the 3D views of the k-DOS distributions on the α-Fermi surfaces in $CeCoIn_5$. This Fermi surface is situated in the four corner of the Brillouin zone. It is clear that the best nesting is expected for $\mathbf{Q} = (q, q, 0.5) = (0.5 \pm \delta q, 0.5 \pm \delta q, 0.5)$ in reciprocal units, where q is evaluated geometrically as $q = 2k_F$ and $1 - 2k_F$. One of $\mathbf{Q}$ is indicated by arrows in Fig. 3. The k_z component of $\mathbf{Q}$ comes from the warping of the α-Fermi surface along the k_z direction. In fact, the joint density of states (JDOS) defined by $N_J(\mathbf{q}) = \langle N(\mathbf{k}, E = 0) N(\mathbf{q} - \mathbf{k}, E = 0) \rangle_{\mathbf{k}}$ is one of the indicators to check the degree of the nesting condition, and its maximum position may signify $\mathbf{Q}$ of the SDW instability. In the JDOS presented in Fig. 3(b), the optimal nesting vector appears at $Q = (0.5 \pm \delta q, 0.5 \pm \delta q, 0.5)$. We obtain $\delta q = 0.05$ when we approximate the Fermi wave number as $k_F = 0.275$, corresponding to the α-Fermi surface, according to the combined efforts by the dHvA experiment and band calculation.[26] According to the NMR experiments[19–21] the observed SDW spectra with the double horn shape for the In(2a) site definitely show that the SDW is characterized by the single Q state, indicating that one of the two pairs for possible nesting vectors is chosen after the SDW instability. The theoretical analysis of those experimental facts belongs to future works.

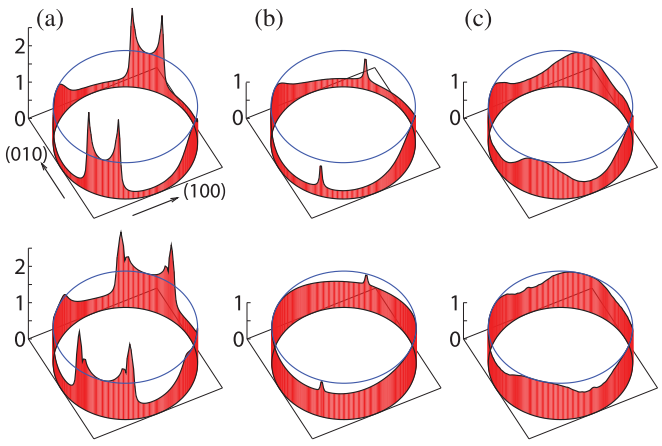

FIG. 2. (Color online) k-DOS $N(\mathbf{k}, E = 0)/N_0$ for low field (upper panels) and high field (lower panels) at $k_z = 0$. (a) For $H \parallel (110)$ with strong Pauli effect $\mu = 2.0$. $H/H_{c2} = 0.74$ (upper) and 0.99 (lower). (b) For $H \parallel (110)$ in the absence of Pauli effect $\mu = 0$. $H/H_{c2} = 0.36$ (upper) and 0.86 (lower). (c) For $H \parallel (001)$ with $\mu = 2.0$. $H/H_{c2} = 0.77$ (upper) and 0.98 (lower). Height of the upper rings indicates the normal state value N_0. $T/T_c = 0.05$.

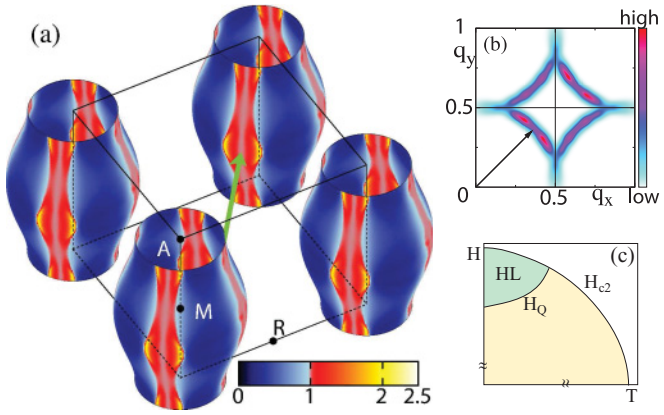

FIG. 3. (Color online) (a) k-DOS distribution drawn on the Fermi surfaces situated on the four corners of the Brillouin zone. $H/H_{c2} = 0.86$, $T/T_c = 0.05$, $H \parallel (110)$, and $\mu = 2$. The arrow indicates a nesting vector $\mathbf{Q}$ connecting large k-DOS positions. (b) Corresponding joint DOS $N_J(\mathbf{q})$ in $0 < q_x, q_y < 1.0$ at $q_z = 0.5$. It indicates four maxima at $\mathbf{Q} = (0.5 \pm \delta q, 0.5 \pm \delta q, 0.5)$ centered around (0.5,0.5,0.5). The arrow denotes one of $\mathbf{Q}$. (c) Schematic experimentally observed phase diagram of the HL phase.

An SDW instability with the nesting vector **Q** could occur at $H_Q(T) < H < H_{c2}$ [see Fig. 3(c) for schematic experimentally observed phase diagram]. As H increases toward H_{c2}, the k-DOS enhancement by vortices becomes larger only along the nodal direction and provides the best SDW nesting condition. The SDW occurs through the repulsive interaction U between QPs induced by vortices, when Stoner instability condition $U\chi(\mathbf{Q}) > 1$ is fulfilled. $\chi(\mathbf{Q})$ is static susceptibility for wave number **Q**. Note that $\chi(\mathbf{Q}=0) = \mu_B^2 N_0$. The in-plane anisotropy of the transition line $H_Q(T)$ may not be large because the total DOSs for two directions (100) and (110) differ only by at most 0.4%.[10] As increasing T under a fixed H, the peak value of the k-DOS enhancement $N(k, E=0)$ decreases because of thermal broadening of the singularities of k-DOS, namely $\chi(\mathbf{Q})$ is enhanced on decreasing T. Thus $dH_Q(T)/dT > 0$, coinciding with the observation.[17] Likewise impurities easily kill the singularities, thus the doping experiment can be understood where the HL phase area diminishes upon small Cd and Hg dopings.[28] The tilting field toward the c axis ceases to induce the k-DOS enhancement above N_0. This is supported by recent neutron experiment[29] and by Correa *et al.*[27] Therefore the HL phase in the in-plane field is not connected to the HL phase in the c-axis field, implying that the latter cannot be an SDW instability, but may be genuine Fulde-Ferrell-Larkin-Ovchinnikov (FFLO). Those are predictions based on our microscopic calculations.

Since the observed wave length of the SDW modulation is an order of ∼5 nm and much shorter than $\xi \sim 30$ nm, there is still a possibility for FFLO to occur as advocated by several authors[12–16] because the present SDW polarized along the c axis[2,3] is compatible with the appearance of FFLO whose polarization occurs along the in-plane field direction. In other words, those two long-range orders are mutually coexisting but independent as a first approximation.

In summary, by solving the microscopic Eilenberger equations self-consistently for $d_{x^2-y^2}$ pairing superconductors with strong Pauli paramagnetic effect, we obtain the detailed information about quasiparticle structures in both real and reciprocal spaces for vortex lattice states. This complementary information allows us to draw a picture that momentum-resolved DOS for the nodal direction in **k** space is enhanced by vortices under in-plane fields and exceed the normal state value. Thus this signals an SDW instability with ordering vector directed toward the nodal direction. This kind of coexistence between SDW and SC with vortices is a form confined exclusively inside the SC phase [see Fig. 3(c)], which is a coexistence scheme where two orderings compete with each other to try to open their own energy gaps on the Fermi surface.[30] The proposed SDW mechanism may apply other heavy Fermion superconductors such as Ce_2PdIn_8.[31]

The authors are grateful for insightful discussions with M. Kenzelmann, S. Gerber, J.S. White, J.L. Gavilano, T. Sakakibara, E.M. Forgan, K. Kumagai, R. Ikeda, V. Mitrovic, N. Curro, and Y. Yanase.

[1] C. Pfleiderer, Rev. Mod. Phys. **81**, 1551 (2009).
[2] M. Kenzelmann *et al.*, Science **321**, 1652 (2008).
[3] M. Kenzelmann *et al.*, Phys. Rev. Lett. **104**, 127001 (2010).
[4] B. Lake *et al.*, Nature (London) **415**, 299 (2002); J. Chang *et al.*, Phys. Rev. Lett. **102**, 177006 (2009).
[5] G. Knebel, D. Aoki, and J. Flouquet, e-print arXiv:0911.5223.
[6] A. A. Abrikosov, Soviet Phys-JETP **5**, 1174 (1957).
[7] M. Ichioka, A. Hasegawa, and K. Machida, Phys. Rev. B **59**, 184 (1999).
[8] H. F. Hess, R. B. Robinson, R. C. Dynes, J. M. Valles Jr., and J. V. Waszczak, Phys. Rev. Lett. **62**, 214 (1989); N. Nakai, P. Miranović, M. Ichioka, H. F. Hess, K. Uchiyama, H. Nishimori, S. Kaneko, N. Nishida, and K. Machida, *ibid.* **97**, 147001 (2006).
[9] A. D. Bianchi *et al.*, Science **319**, 177 (2008).
[10] K. An, T. Sakakibara, R. Settai, Y. Onuki, M. Hiragi, M. Ichioka, and K. Machida, Phys. Rev. Lett. **104**, 037002 (2010).
[11] K. Izawa, H. Yamaguchi, Y. Matsuda, H. Shishido, R. Settai, and Y. Onuki, Phys. Rev. Lett. **87**, 057002 (2001).
[12] A. Aperis, G. Varelogiannis, and P. B. Littlewood, Phys. Rev. Lett. **104**, 216403 (2010).
[13] D. F. Agterberg, M. Sigrist, and H. Tsunetsugu, Phys. Rev. Lett. **102**, 207004 (2009).
[14] Y. Yanase and M. Sigrist, J. Phys. Soc. Jpn. **78**, 114715 (2009).
[15] K. Miyake, J. Phys. Soc. Jpn. **77**, 123703 (2008).
[16] R. Ikeda, Y. Hatakeyama, and K. Aoyama, Phys. Rev. B **82**, 060510(R) (2010).
[17] A. Bianchi, R. Movshovich, C. Capan, P. G. Pagliuso, and J. L. Sarrao, Phys. Rev. Lett. **91**, 187004 (2003).
[18] K. Kakuyanagi, M. Saitoh, K. Kumagai, S. Takashima, M. Nohara, H. Takagi, and Y. Matsuda, Phys. Rev. Lett. **94**, 047602 (2005).
[19] G. Koutroulakis, V. F. Mitrović, M. Horvatić, C. Berthier, G. Lapertot, and J. Flouquet, Phys. Rev. Lett. **101**, 047004 (2008).
[20] B.-L. Young, R. R. Urbano, N. J. Curro, J. D. Thompson, J. L. Sarrao, A. B. Vorontsov, and M. J. Graf, Phys. Rev. Lett. **98**, 036402 (2007).
[21] G. Koutroulakis, M. D. Stewart Jr., V. F. Mitrović, M. Horvatić, C. Berthier, G. Lapertot, and J. Flouquet, Phys. Rev. Lett. **104**, 087001 (2010).
[22] T. Watanabe *et al.*, Phys. Rev. B **70**, 020506(R) (2004).
[23] K. Kumagai *et al.*, Phys. Rev. Lett. **97**, 227002 (2006).
[24] H. Aoki, T. Sakakibara, H. Shishido, R. Settai, Y. Onuki, P. Miranović, and K. Machida, J. Phys. Condens. Matter **16**, L13 (2004).
[25] M. Ichioka and K. Machida, Phys. Rev. B **76**, 064502 (2007).
[26] H. Shishido *et al.*, J. Phys. Soc. Jpn. **71**, 162 (2002).
[27] V. F. Correa *et al.*, Phys. Rev. Lett. **98**, 087001 (2007).
[28] Y. Tokiwa *et al.*, Phys. Rev. Lett. **101**, 037001 (2008).
[29] E. Blackburn *et al.*, Phys. Rev. Lett. **105**, 187001 (2010).
[30] K. Machida and M. Kato, Phys. Rev. Lett. **58**, 1986 (1987); K. Machida, J. Phys. Soc. Jpn. **50**, 2195 (1981); K. Machida and T. Matsubara, *ibid.* **50**, 3231 (1981).
[31] J. K. Dong *et al.*, e-print arXiv:1008.0679.